Long-Term Seaport Activity Monitoring with Sentinel-1 Polarimetric SAR Imagery

Morton J. Canty

Heinsberger Str. 18, D-52428 Jülich, Germany

Abstract

abstract ...

Keywords: remote sensing, synthetic aperture radar, statistical testing, sequential change detection, cloud computing

1. Introduction

Synthetic Aperture Radar (SAR) is being widely used for monitoring purposes over many areas of interest throughout the world. The Sentinel-1 SAR space mission operated by the European Space Agency offers free access to the sensor data, unlike some other radar imagery suppliers that charge fees for each dataset. A convenient and near-real-time source of time-sequential SAR data is provided by the Google Earth Engine (GEE) platform (**?**) which archives Sentinel-1 dual polarimetric SAR images as soon as they are made available by the European Space Agency. The GEE also offers a platform to design and execute algorithms on remote sensing datasets through cloud services, thus relinquishing user's local network from the burden of data storage and processing.

This paper describes the application of a sequential change detection algorithm to time series of Sentinel-1 images over the Port of Long Beach and Los Angeles, the object being to track the effect of erratically declared American tariffs since the beginning of the Trump administration on west coast shipping activity. Long Beach / Los Angeles is the busiest seaport in

the western hemisphere and one of the busiest in the world, approximately 15,000 longshore workers usually pull shifts around the clock, moving billions of dollars' worth of cargo in cars, agriculture, auto parts, toys, clothes and furniture. It thus offers itself as an ideal indicator of major shifts in international trade involving the USA.

The algorithm used in the study is based on an omnibus likelihood ratio test statistic for the equality of several variance-covariance matrices (**?**). It enables geospatial and temporal isolation of changes in a time series of multi-look SAR data in polarimetric matrix representation, with single polarization and diagonal-only intensity data included as a special cases. The ability of the sequential change detection method to detect and isolate regions of intense activity, together with easy access to Sentinel-1 SAR imagery on the GEE, suggest specific applications in the area of remote monitoring. The change detection method, including open source change detection software for interaction with the GEE is described in in Chapter 9 of **?** and summarized below. The software is available on GitHub and the client-side programs run in a local Docker container.

2. Theory

The term "multi-look" in SAR imagery refers to the number of independent observations of a surface pixel area that have been averaged in order to reduce the effect of speckle, a noise-like consequence of the coherent nature of the radar signal emitted from the sensor. In the case of polarimetric SAR, the observed signals are multivariate complex Gaussian distributed and their variance-covariance representations, when multiplied by the number of looks, are correspondingly complex Wishart distributed. This distribution is the multivariate complex analogue of the well-known chi-square distribution for the variance of Gaussian-distributed scalar observations.

The complex Wishart distribution is completely determined by the parameter Σ (the covariance matrix) and by the *equivalent number of looks* ENL. The latter is the number of looks corrected for the lack of indepen-

dence of the multi-look observations. Given two measurements of polarized backscatter from the same region on the ground surface at different times, one can set up a so-called hypothesis test in order to decide whether or not a change has occurred. The null hypothesis is that $\Sigma_1 = \Sigma_2$, i.e., the two observations were sampled from the same distribution and no change has occurred, and the alternative hypothesis is $\Sigma_1 \neq \Sigma_2$, in other words, there was a change (the ENL is assumed to be the same in both images). Since the distributions are known, a likelihood ratio test can be formulated which allows one to decide to a desired degree of significance whether or not to reject the null hypothesis. Acceptance or rejection is based on the so-called p-value, the probability of getting a test statistic that is at least as extreme as the one observed, given the null hypothesis. The p-value may be derived from the (approximately known) distribution of the likelihood ratio test statistic. In the case of $k > 2$ observations this procedure can be generalized to test a null hypothesis that all of the k pixels are characterized by the same Σ, against the alternative that at least one of the Σ_i , $i = 1 \ldots k$, are different, i.e., that at least one change has taken place. Furthermore this so-called *omnibus test procedure* can be factored into a sequence of tests involving hypotheses of the form:

$$\Sigma_1 = \Sigma_2 \text{ against } \Sigma_1 \neq \Sigma_2$$

$$\Sigma_1 = \Sigma_2 = \Sigma_3 \text{ against } \Sigma_1 = \Sigma_2 \neq \Sigma_3$$

and so forth. The tests are statistically independent under the null hypothesis. In the event of rejection of the null hypothesis at some point in the test sequence, the procedure is restarted from that point, so that multiple changes within the time series can be identified.

2.1. Dual polarization, diagonal only

To be more specific, we describe below the hypothesis tests for dual pol, diagonal only, polarimetric matrices. The per-pixel observations are expressed as multi-look polarimetric matrices which, in the case of vertical

emission, vertical and horizontal reception, have the form

$$\bar{C} = \begin{pmatrix} \langle |S_{vv}|^2 \rangle & \langle S_{vv} S_{vh}^* \rangle \\ \langle S_{vh} S_{vv}^* \rangle & \langle |S_{vh}|^2 \rangle \end{pmatrix},$$

where S_{vv} is the complex scattering amplitude for vertically polarized emission and detection, S_{vh} for vertical emission horizontal reception. The angular brackets denote multi-looking. The Earth Engine database only archives the diagonal matrix elements, not the (complex) off-diagonal elements, so in fact one works with observations of the form

$$\bar{C} = \begin{pmatrix} \langle |S_{vv}|^2 \rangle & 0 \\ 0 & \langle |S_{vh}|^2 \rangle \end{pmatrix}.$$

If we write

$$x = m\bar{C}$$

where m is the equivalent number of looks, then the omnibus test for

$$H_0 : \quad \Sigma_1 = \Sigma_2 = \ldots = \Sigma_k = \Sigma,$$

against

$$H_1 : \quad \Sigma_i \neq \Sigma_j \text{ for at least one pair } i, j$$

has the critical region

$$Q = k^{2km} \frac{|x_1|^m |x_2|^m \cdots |x_k|^m}{|x_1 + x_2 + \ldots x_k|^{km}} \leq t.$$

The left hand side of the inequality is the ratio of the maximum likelihood of observing the data under the null hypothesis to that of observing the data irrespective of change. If the ratio is less than some threshold t, then the null hypothesis is rejected. Taking logarithms:

$$\ln Q = m(2k \ln k + \sum_{i=1}^{k} \ln |x_i| - k \ln |\sum_{i=1}^{k} x_i|) \leq t'.$$

We have the following approximation for the statistical distribution of the test statistic Q:

$$\text{prob}(-2 \ln Q \leq z) \simeq P_{\chi^2;2(k-1)}(z)$$

where $P_{\chi^2;f}(z)$ is the chi-square distribution with f degrees of freedom. In practice we choose a significance level α, e.g., $\alpha = 0.001$, and reject the null or no-change hypothesis when the p value satisfies

$$p = 1 - P_{\chi^2;2(k-1)}(-2\ln Q) < \alpha.$$

2.2. Sequential omnibus test

As mentioned above, the omnibus test can be factored into a sequence of tests involving hypotheses of the form $\Sigma_1 = \Sigma_2$ against $\Sigma_1 \neq \Sigma_2$, $\Sigma_1 = \Sigma_2 = \Sigma_3$ against $\Sigma_1 = \Sigma_2 \neq \Sigma_3$, and so forth. For example, to test

$$H_{0j}: \quad \Sigma_1 = \Sigma_2 = \ldots \Sigma_{j-1} = \Sigma_j$$

against

$$H_{0j}: \quad \Sigma_1 = \Sigma_2 = \ldots \Sigma_{j-1} \neq \Sigma_j$$

the likelihood ratio test statistic is R_j^1 given by

$$\ln R_j^1 = m[N(j\ln j-(j-1)\ln(j-1))+(j-1)\ln|\sum_{i=1}^{j-1}x_i|+\ln|x_j|-j\ln|\sum_{i=1}^{j}x_i|\,],$$

for $j = 2 \ldots k$, and

$$\text{prob}(-2\ln R_j^1 \leq z) \simeq P_{\chi^2;2}(z).$$

The null hypothesis correspondingly rejected when

$$p = 1 - P_{\chi^2;2}(-2\ln R_j^1) < \alpha.$$

Moreover the R_j^1 constitute a factorization of Q such that $Q = \prod_{j=2}^{k} R_j^1$, or

$$\ln Q = \sum_{j=2}^{k} \ln R_j^1.$$

and the tests are statistically independent under the null hypothesis.

Now suppose that we conclude $\Sigma_1 \neq \Sigma_2$. Then we can continue to look for additional changes by restarting the tests at $j = 3$,

$$\ln R_j^2 = m[N(j\ln j-(j-1)\ln(j-1))+(j-1)\ln|\sum_{i=2}^{j-1}x_i|+\ln|x_j|-j\ln|\sum_{i=2}^{j}x_i|\,],$$

for $j = 3 \ldots k$. This procedure is continued until the end of the image sequence.

2.3. Computation strategy

Denoting the test statistics $R_j^\ell,\ \ell = 1 \ldots k-1,\ j = \ell+1 \ldots k$, for a series of, say, $k = 5$ images, we have the following tests to consider

ℓ/j	2	3	4	5
1	R_2^1	R_3^1	R_4^1	R_5^1
2		R_3^2	R_4^2	R_5^2
3			R_4^3	R_5^3
4				R_5^4

For example, if the test R_2^1 does not reject H_0, but test R_3^1 does, then the subsequent tests R_4^1 and R_5^1 in the first row are irrelevant. We re-start the sequence in row 3 at R_4^3 and continue to check for additional change. From a computational standpoint, since the test sequences must be applied to every pixel, it is advantageous to pre-calculate all of the p-values (in this example there are 10 of them) irrespectively of their relevance. Then, in a second pass over the p-value arrays, the valid changes are identified. This is the strategy adopted in the implementation of the sequential omnibus algorithm on the GEE Python API: The p-value arrays are pre-computed and then scanned at the desired significance level. Four one–byte arrays having the spatial dimensions of the images are updated recursively in order to generate geo-referenced change maps. These are:

- c_map: the interval in which the most recent significant change occurred (single-band)
- s_map: the interval in which the first significant change occurred (single-band)
- f_map: the frequency of significant changes (single-band)
- b_map: the interval in which each significant change occurred ($(k-1)$-band).

The f_map is particularly advantageous for identifying small regions of concentrated activity over the time sequence, while the b_map can be used to determine change profiles of specific regions of interest and to generate change animations and activity plots.

cov

3. Port of Long Beach and Los Angeles

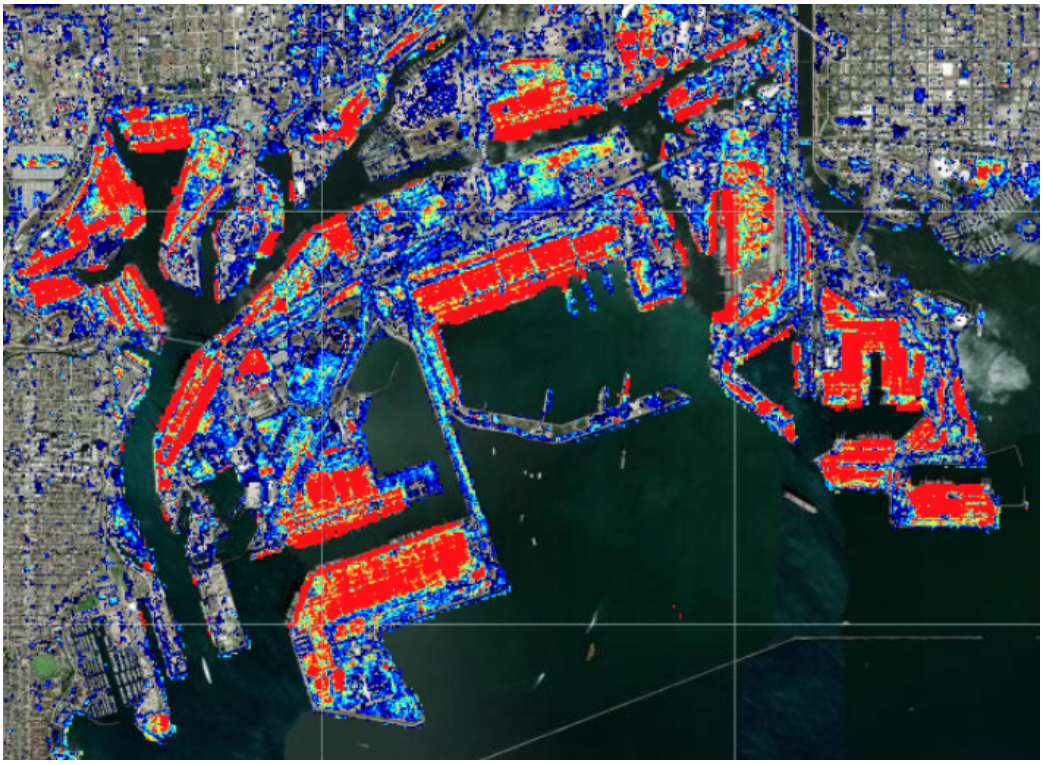

Figure 1: Fraction of changes per pixel from Jan. 2022 through May 2025 excluding water surface. Dark blue: few. Red: more than 20.

"The US West Coast gateway ports of Los Angeles and Long Beach saw a surge in container volumes in January 2023 as retailers restocked inventory ahead the Lunar New Year shutdown in China." (Seatrade Maritime News, Feb. 15, 2024)

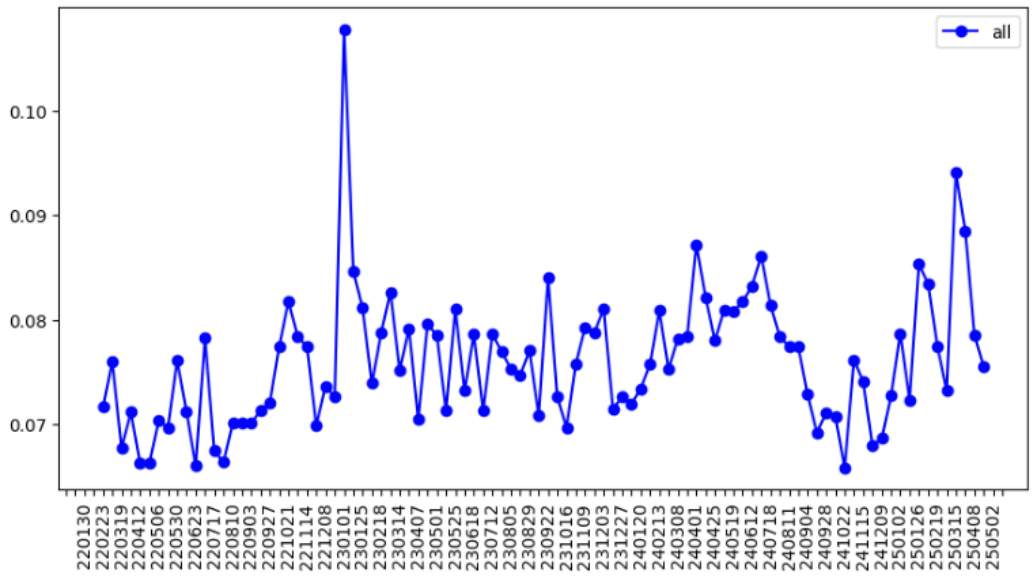

Figure 2: Number of changes per interval.

Figure 3: Middle Harbor Terminal (Pier T) "Operated by COSCO Shipping (OOCL) and Long Beach Container Terminal (LBCT) Primary Chinese Connection: COSCO Shipping (China Ocean Shipping Company) has a significant presence here." (deepseek)

4. Conclusions

some nice conclusions

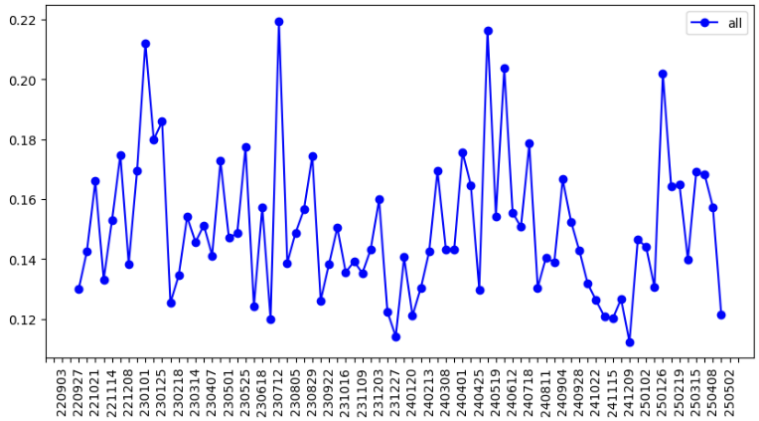

Figure 4: Middle Harbor Terminal (Pier T) changes

References